doi:10.1017/S1431927613005540
Microsc. Microanal. 19 (Suppl 2), 2013

Measuring Lattice Parameters and Local Rotation using Convergent Beam Electron Diffraction: One Step Further

Yannick Martin[1], Jian-Min Zuo[2], Vincent Favre-Nicolin[1,3], Jean-Luc Rouvière[1]

[1.] CEA-INAC/UJF-Grenoble1 UMR-E, SP2M, Minatec 17 rue des Martyrs 38054 Grenoble France
[2.] Department of Material Science and Engineering and Materials Research Laboratory, University of Illinois at Urbana-Champaign, Urbana, IL 61801, USA
[3.] Université Grenoble-Alpes, F-38041 Grenoble

In this paper, we present a new method to retrieve lattice parameters and local rotation of a crystal using both diffracted and transmitted beams in a Convergent Beam Electron Diffraction (CBED) pattern. The size of the electron probe is about 1 nm, allowing a high special resolution. The lattice can be determined with a relative accuracy of 2×10^{-4} in the plane perpendicular to the beam, and 1×10^{-2} along the beam direction. The rotation is determined with a precision of 0.5 mrad in the plane perpendicular to the beam and 3.10^{-2} mrad along the beam direction (Table 1). This method has been validated using Bloch waves dynamic simulations.

CBED is considered as a promising technique for measuring local small strain in crystalline materials, as the positions of HOLZ lines are very sensitive to small changes in the lattice parameters. Various methods to retrieve lattice strain from recorded CBED patterns have been developed: based on the use of the distances between intersections of HOLZ lines [1], on the fit of HOLZ line positions by using kinematical calculations including a dynamical correction [2][3], on the use of Hough transform, or on the KLEBS method (K-Line Equation Based Scheme) [4]. As the need to correlate the strain and carrier mobility increases in the semiconductor industry [5], CBED became a very popular technique for measuring strain in semiconductor devices. However the broadening of HOLZ lines (also known as HOLZ line splitting) in thin TEM lamellas [6] made the CBED pattern analysis more complex. The proposed method here is a first step towards an improved analysis of CBED patterns that include HOLZ lines broadening.

The proposed method is based on three original ideas. Firstly it uses both deficient and excess HOLZ lines i.e. both transmitted and diffracted beams in order to retrieve local crystal orientation and lattice parameters (previous methods used only the transmitted beam). Secondly, it uses a reference diffraction pattern from which HOLZ shifts can be determined. Thirdly, in fitting experimental patterns, it uses kinematic simulations with HOLZ line shift corrections that are initially calculated in the reference diffraction patterns. In this study, only sharp HOLZ lines are considered.

The algorithm uses positions and angle of about ten deficient HOLZ lines and the position and angle of five to ten excess HOLZ lines. Fitting the position of excess HOLZ lines gives improved accuracy. The positions and angles are fitted using kinematic simulations which includes a HOLZ line shift corrections as state above. We show that for small lattice variations (< 1%) and small crystal rotations (< 10 mrad) this kinematic scheme (kinematic calculations with additional shift corrections) allows to reproduce the variations of HOLZ line positions that have been computed dynamically.

The results have been obtained on dynamically simulated pattern made by the general matrix method (Figure 1). From this diffraction pattern, the lattice parameters and the crystal orientation i.e. 9

parameters, are retrieved by a minimization algorithm. Table 1 gives the retrieval results on eight simulated crystals that have different lattice parameters (varying altogether). During this presentation we will discuss the quantitative results using this new technique as well as its limits.

References:

[1] P.M. Jones, G.M. Rackam, and J.W. Steed, Proc. R. Soc. London A **354** (1977), p. 197-222
[2] J.M. Zuo, Ultramicroscopy **41** (1992), p. 211–223
[3] Y.P. Lin, D.M. Bird, and R. Vincent, Ultramicroscopy **27** (1989), p. 233–240
[4] A. Moraviec, Ultramicroscopy **107** (2007) p. 390–395
[5] F. Schaeffler, Semiconductor Science and Technology **12** (1997) p.1515–1549.
[6] L. Clément et al., Appl. Phys. Lett. **85** (2004), p. 651

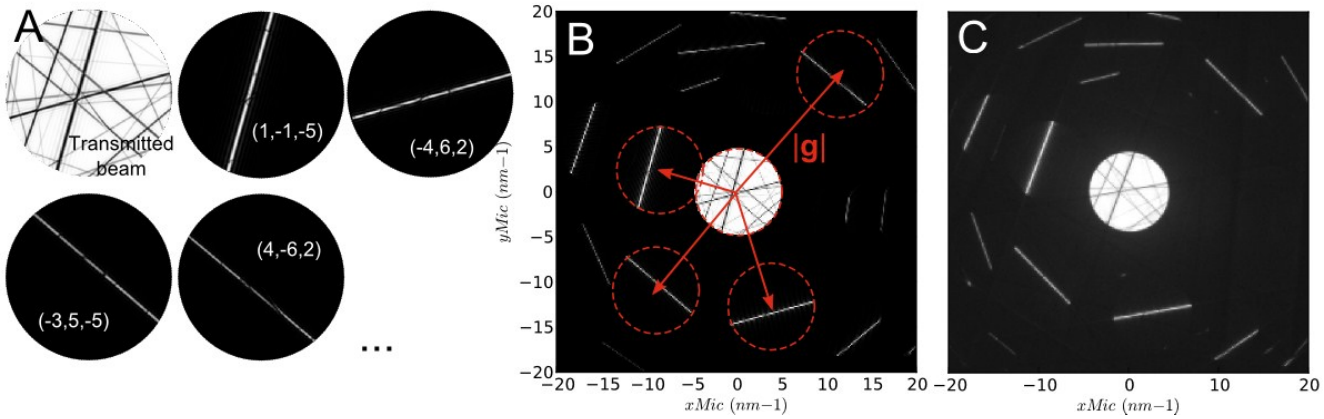

Figure 1. A-1kx1k Dynamically simulated beams B-Reconstruction of the whole dynamic CBED pattern, C-Experimental pattern (Voltage 200kV, zone axis [651,441,31], perfect silicon)

Table 1. Results of the strain retrieval on eight different crystal parameters. g_x, g_y are perpendicular to the beam, g_z parallel. $\alpha_\perp$ is the angle between g_x and g_y. $\beta_\parallel$ (resp. $\gamma_\parallel$) is the angle between g_x (resp. g_y) and g_z. For small strain (<1%) the precision is 2×10^{-4} inside the plane, 1×10^{-2} outside (g_z seems to be well fitted but the angles $\beta_\parallel$, $\gamma_\parallel$ are not precise). For higher strains the precision decreases. The rotation is very well fitted outside the plane ($\Delta\Phi_\perp$<3.10^{-2} mrad) and well fitted inside the plane ($\Delta\Phi_\parallel$< 0.5mrad).

Variation of crystal parameters (%)						*Precision of retrieved parameters*							
$\frac{\Delta a}{a_0}$	$\frac{\Delta b}{b_0}$	$\frac{\Delta c}{c_0}$	$\frac{\Delta \alpha}{\alpha_0}$	$\frac{\Delta \beta}{\beta_0}$	$\frac{\Delta \gamma}{\gamma_0}$	$\frac{\Delta g_x}{g_x}$	$\frac{\Delta g_y}{g_y}$	$\frac{\Delta g_z}{g_z}$	$\frac{\Delta \alpha_\perp}{\alpha_\perp}$	$\frac{\Delta \beta_\parallel}{\beta_\parallel}$	$\frac{\Delta \gamma_\parallel}{\gamma_\parallel}$	$\Delta\Phi_\parallel$ (mrad)	$\Delta\Phi_\perp$ (mrad)
0 = reference perfect crystal						-1.9e-7	2.0e-7	-1.3e-8	-2.5e-5	-4.0e-4	6.5e-4	1.55e-3	-0.44
-0.05	-0.1	0.05	-0.25	0.15	-0.1	-9.3e-6	1.3e-4	-1.2e-4	-4.2e-4	-1.0e-2	2.0e-3	1.97e-2	-0.16
-0.15	-0.3	0.15	-0.75	0.45	-0.3	-7.6e-5	2.4e-5	5.2e-5	-5.1e-4	-3.6e-3	7.9e-3	5.83e-3	-0.10
-0.3	-0.6	0.3	-1.5	0.9	-0.6	-1.0e-4	1.9e-4	-9.0e-5	-7.8e-4	-1.2e-2	5.8e-3	1.60e-2	-0.13
-0.4	-0.8	0.4	-2.0	1.2	-0.8	-9.8e-5	2.2e-4	-1.2e-4	-6.5e-4	-1.4e-2	4.2e-3	3.19e-2	0.11
-0.5	-1.0	0.5	-2.5	1.5	-1.0	-2.5e-4	1.6e-4	9.6e-5	-6.2e-4	-1.1e-2	1.0e-2	9.05e-3	0.28
-0.65	-1.3	0.65	-3.2	2.0	-1.3	-3.6e-4	2.8e-4	8.0e-5	-3.5e-4	-1.6e-2	1.2e-2	2.88e-2	0.26
-0.8	-1.6	0.8	-4.0	2.4	-1.6	-7.8e-4	5.1e-4	2.7e-4	-1.2e-3	-1.9e-2	1.8e-2	1.96e-2	1.16
-0.9	-1.8	0.9	-4.5	2.7	-1.8	-2.0e-4	4.3e-4	1.5e-4	-1.8e-4	-7.3e-3	5.4e-3	2.50e-2	-0.10

https://doi.org/10.1017/S1431927613005540 Published online by Cambridge University Press